Frontiers in Bioscience Landmark

Front. Biosci. (Landmark Ed) **2025**; 30(8): 45142
https://doi.org/10.31083/FBL45142

Original Research

Biomembranal Myristoyl-Phosphatidylcholine as a Potential Target of the Cell Injury Activity of Vitamin D Decomposition Products in Eukaryotic Cells

Hirofumi Shimomura[1,*], Kiyofumi Wanibuchi[2], Kouich Hosoda[3], Avarzed Amgalanbaatar[4], Mitsuru Shoji[2], Shunji Hayashi[1]

[1]Department of Microbiology, School of Medicine, Kitasato University, Sagamihara-shi, 252-0374 Kanagawa, Japan
[2]Faculty of Pharmaceutical Sciences, Yokohama University of Pharmacy, Yokohama-shi, 245-0066 Kanagawa, Japan
[3]Processing for Distribution of Heiwajima, Manufacturing Team, Group of Product Procurement, Promotion Office of SCM, Terumo Co., 143-0006 Tokyo, Japan
[4]Department of Graduate Education, Graduate School, Mongolian National University of Medical Sciences, 14210 Ulaanbaatar, Mongolia
*Correspondence: shimomura.hirofumi@kitasato-u.ac.jp (Hirofumi Shimomura)
Academic Editor: Xiaolei Tang
Submitted: 19 July 2025 Revised: 14 August 2025 Accepted: 21 August 2025 Published: 30 August 2025

Abstract

Background: Vitamin D decomposition products target a myristic acid sidechain of the predominant glycerophospholipid constructed in the biomembranes of *Helicobacter pylori,* causing gastric cancer in humans, and disrupt the membrane structure, followed by bacteriolysis. No earlier studies, however, elucidate whether vitamin D decomposition products interact with the glycerophospholipids that construct the eukaryotic biomembranes and confer whatever cell disorders. **Methods**: A gastric cancer cell line, MKN45, and a non-cancer cell line, Vero, were used in this study. Cell injury activities of vitamin D decomposition products (VDP1 and VD2-1) and a VDP1 derivative (VD3-7) were examined by the 3-(4,5-di-methylthiazol-2-yl)-2,5-diphenyltetrazolium bromide (MTT) assay. Identification of a glycerophospholipid was performed by ^{1}H-nuclear magnetic resonance (NMR). Fatty acid composition and glycerophospholipid molecular species were analyzed by gas chromatography/mass spectrometry (GC/MS) and liquid chromatography/mass spectrometry (LC/MS), respectively. Structure collapse-induction activity of VDP1, VD2-1 and VD3-7 to glycerophospholipid vesicles was examined using the pigment-containing lamellar vesicles. **Results**: MKN45 cells exhibited higher susceptibility to the cell injury activity of VDP1 and VD2-1 than Vero cells. In the analysis of biomembrane lipids, the glycerophospholipid phosphatidylcholine (PC) molecular species turned out to conspicuously differ between MKN45 cells and Vero cells. Contents of myristoyl-PC were higher in MKN45 cells than in Vero cells, while contents of oleoyl-PC were higher in Vero cells than in MKN45 cells. Meanwhile, the contents of palmitoyl- and palmitoleoyl-PC were almost equal between these cells. We next examined the structure collapse-induction activity of VDP1, VD2-1 and VD3-7 on the lamellar vesicles prepared with dimyristoyl-PC, dipalmitoyl-PC and dioleoyl-PC. The vitamin D decomposition products and a VDP1 derivative induced the structural collapse of dimyristoyl- and dipalmitoyl-PC lamellar vesicles but almost no structural collapse of dioleoyl-PC lamellar vesicles. These results suggest that the contents of myristoyl-PC in biomembranes are associated with the susceptibility of eukaryotic cells to the cell injury activity of VDP1, VD2-1 and VD3-7. In addition, no VD3-7 affected the viability of Vero cells and selectively decreased the viability of MKN45 cells. **Conclusions**: In the future, we will expect to be capable of developing novel antitumor agents targeting the myristic acid sidechain of biomembranal PC using a vitamin D decomposition product as the fundamental structure.

Keywords: vitamin D; phosphatidylcholines; myristic acid; eukaryotic cells

1. Introduction

Vitamin D is a hormone generated from steroidal compounds such as ergosterol and 7-dehydrocholesterol. Ergosterol and 7-dehydrocholesterol are precursors of vitamins D_2 and D_3, respectively [1]. Vitamins D metabolized to the activation form exhibit various hormonal actions in the exogenous calcium ion incorporation, bone metabolism and innate immune system. Apart from this, a previous study by our group demonstrated that the decomposition products obtained from abiotic degradation of vitamin D_3 confer more potent bactericidal action to *Helicobacter pylori,* causing gastritis, peptic ulcers and gastric cancers in humans [2–4] than the intact vitamin D_3 [5]. We, therefore, identified with a vitamin D_3 decomposition product, VDP1, that potently induces bacteriolysis in *H. pylori*. VDP1 is an indene compound arranged a carbonyl and an alkyl in the frame. As with VDP1, a vitamin D_2 decomposition product, VD2-1, also acts as a significant bactericidal agent on *H. pylori* [6,7]. VDP1 and VD2-1 are considered to bind to the characteristic glycerophospholipids comprising the biomembranes of *H. pylori*, to induce the structural change to a myristic acid sidechain of its glycerophospholipid, to thereby destabilize the bacterial membrane conformation, and to ultimately lead this pathogen to lysis [8]. In sum,

we elucidated the biological activity of vitamin D decomposition products in a prokaryote. Meanwhile, no earlier studies, however, examine whether vitamin D decomposition products exhibit whatever biological activities in eukaryotic cells. In this study, we investigate the cell injury activity of VDP1 and VD2-1 to gastric cancer cells and describe the possibility of the development of novel antitumor medicines using VDP1 and VD2-1 as fundamental structures.

2. Materials and Methods

2.1 VDP1, VD2-1 and VD3-7

After a condensation product was generated by an aza-Diels-Alder reaction of vitamin D and 4-phenyl-1,2,4-triazoline-3,5-dione (PTAD), VDP1 and VD2-1 (Fig. 1) were chemically synthesized via an oxidation reaction of the condensation product using a ruthenium chloride-periodate [6,7]. VD3-7 was a VDP1 derivative with a carbonyl substituted to a fluorine in the VDP1 molecule [7].

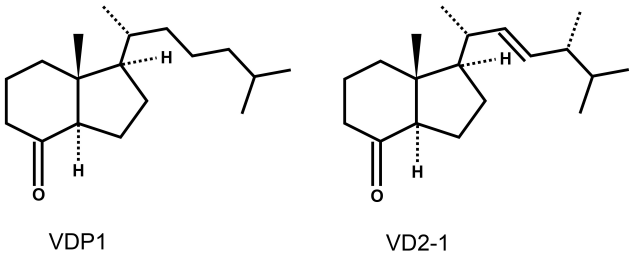

Fig. 1. Chemical structures of VDP1 and VD2-1. VDP1, (1R,3aR,7aR)-1-[(1R)-1,5-dimethylhexyl]octahydro-7a-methyl-4*H*-inden-4-one; VD2-1, ((1*R*,3a*R*,7a*R*)-1-((2*R*,*E*)-5,6-dimethylhept-3-en-2-yl)-7a-methyloctahydro-4*H*-inden-4-one.

2.2 Cell Lines and Cultures

This study examined two cell lines, MKN45 cells (GeneticLab Co., Ltd., Sapporo, Japan) and Vero cells (a donation item from Yuichi Ishida of Vaxxinova K.K.), that had been maintained in our laboratory. MKN45 cells are a poorly differentiated adenocarcinoma cell line obtained from the human stomach, and Vero cells are a non-cancer epithelial cell line obtained from the kidney of the African green monkey. These cell lines are commercially available, and the strain numbers of the MKN45 cell line and the Vero cell line are JCRB0254 and RCB0001, respectively. The cells were cultured in RPMI 1640 (Sigma-Aldrich Inc., St. Louis, MO, USA) medium supplemented with 10% heat-inactivated fetal calf serum (ThermoFisher Scientific Inc., Tokyo, Japan), 10 mM HEPES (ThermoFisher Scientific Inc., Tokyo, Japan) and 2 mM L-glutamine at 37 °C in a humidified 5% CO_2 incubator. Incidentally, the cell lines used in this study were validated by a short tandem repeat (STR) profiling and tested negative for mycoplasma.

2.3 Assay of Cell Injury Activity

After washing once with phosphate-buffered saline (PBS) by centrifugation, the cell suspension (100 µL) adjusted to 4×10^6 cells/mL using the culture medium was inoculated into the same culture medium (100 µL) containing various concentrations of either VDP1, VD2-1 or VD3-7 and incubated for 24 h at 37 °C in the CO_2 incubator. After a 20 µL volume of 3-(4,5-di-methylthiazol-2-yl)-2,5-diphenyltetrazolium bromide (MTT) (Sigma-Aldrich Inc., St. Louis, MO, USA) reagent (5 mg/mL in PBS) was added to the cell culture, the cell suspension was further incubated for 2 h under the same conditions and the supernatant was removed. The formazan blue, a MTT metabolite crystalizing only in viable cells, was solubilized in an isopropanol solution (200 µL) containing 5% formic acid, and the absorbance ($A_{540\ nm}$) of the formazan blue solution (150 µL) was measured at a wavelength of 540 nm. Viability of the cells incubated in the presence of either VDP1, VD2-1 or VD3-7 was calculated by relative $A_{540\ nm}$ against the $A_{540\ nm}$ in the cells incubated in the absence of VDP1, VD2-1 and VD3-7. Half maximum inhibitory concentrations (IC_{50}) were expressed with the concentrations of VDP1, VD2-1 and VD3-7 that had reduced the $A_{540\ nm}$ values to the half values when $A_{540\ nm}$ value in the cells without VDP1, VD2-1 and VD3-7 was converted into a relative value.

2.4 Extraction of Lipids

After washing three times with PBS by centrifugation, the cell pellets were suspended in distilled water (8 mL), added into chloroform–methanol (2:1) mixture solvents (40 mL) in a glass bottle, vigorously shaken in the bottle and incubated overnight at 4 °C. After the upper solution was removed, solvent of the lower solution was vaporized at 60 °C by a rotary-evaporator (Nihon Büchi K.K., Tokyo, Japan) in order to obtain lipids. After the dry weight of lipids was measured, lipids (approximately 15 mg) were solubilized in a chloroform solvent (1 mL).

2.5 Analysis of Lipids by Thin-Layer Chromatography (TLC)

Lipids (50 µg or 200 µg) dotted onto a silica gel plate (Merck) for TLC were developed on the plate surface together with chloroform–methanol–acetone–water (10:10:1:1) mixture solvents and dried. After a 60% sulfuric acid solution was sprayed on the TLC plate surface, whole lipids were detected by heating the TLC plate at 180 °C. Phospholipids were detected by spraying a Dittmer's reagent on the TLC plate surface.

2.6 Fractionation of Lipids by Silica Gel Column Chromatography

Whole lipids (approximately 15 mg) solubilized in chloroform solvent (1 mL) were put on a column (1-centimeter diameter; 5-centimeter height) filled with

chloroform-activated silica gel beads (Iatrobeads 6RS-8060; Mitsubishi Kagaku Iatron Inc., Tokyo, Japan). Individual lipids were eluted from the column using in the order of chloroform solvent (10 mL), acetone solvent (10 mL), acetone–methanol (9:1) mixture solvents (10 mL), acetone–methanol (8:2) mixture solvents (10 mL), acetone–methanol (7:3) mixture solvents (10 mL), acetone–methanol (6:4) mixture solvents (10 mL), acetone–methanol (5:5) mixture solvents (10 mL), acetone–methanol (4:6) mixture solvents (10 mL), acetone–methanol (3:7) mixture solvents (10 mL) and acetone–methanol (2:8) mixture solvents (10 mL). After eluates were vaporized by a rotary evaporator, lipids were obtained.

2.7 Analysis of Lipids by Proton Nuclear Magnetic Resonance (^{1}H-NMR)

Lipid fractions separated by silica gel column chromatography were dissolved in a deuterated chloroform solvent containing a small amount of tetramethylsilane. A 1,2-dimyristoyl-*sn*-glycero-3-phosphocholine (DMPC) was dissolved in the same solvent and used as a reference lipid species. Lipid solution was put in a ^{1}H-NMR spectrometer ECA500 device (JEOL Ltd., Tokyo, Japan) and chemical-shift signals of the lipids were detected based on the baseline signal (0.0 ppm) of chemical-shift of tetramethylsilane. The following conditions were adopted for the ^{1}H-NMR analysis: resonance frequency, 500.1 MHz; temperature, 23 °C.

2.8 Analysis of Fatty Acid Composition of Phosphatidylcholine (PC)

PC specimen was stirred in methanol solvent (1 mL) containing 5% hydrochloric acid, and then heated for 30 min at 70 °C. After cooling at room temperature, distilled water (1 mL) was added to the solution containing methanolized PC, stirred, and then hexane (1 mL) was added to the solution. After the solution was shaken for 30 s and centrifuged, fatty acid methyl esters derived from PC specimens were obtained from the upper solution. Fatty acid methyl ester solution (1 µL) was injected together with an internal standard palmitic acid-d_{31} methyl ester into a TC70 column (GL Sciences Inc., Tokyo, Japan) equipped with a GCMS-QP2010 Ultra device (Shimadzu Techno-Research Inc., Tokyo, Japan), and spectra of fatty acid methyl ester were detected by an electron ionization mass spectrometry. Fatty acids were identified by comparison to mass spectra of fatty acids registered in a computer database library. Ratio of fatty acid composition was calculated based on the magnitude of the peak area of each fatty acid spectrum.

2.9 Analysis of PC Molecular Species

PC specimen dissolved in chloroform–methanol (1:1) mixture solvents (3 µL) was injected together with an internal standard DMPC-d_{54} into an XBridge C8 column (Waters Co., Tokyo, Japan) equipped to a LC30A Nexera (Shimadzu Techno-Research Inc., Tokyo, Japan)-Triple Quad 5500 (AB Sciex Co., Tokyo, Japan) system device, and spectra of PC molecular species were scanned by an electrospray ionization mass spectrometry with a negative mode. Individual PC molecular species were determined by the fatty acid pairs, which were identified by the analysis of the fatty acid composition. Ratio for each PC molecular species was calculated from the magnitude of the peak area of each mass spectrum.

2.10 Preparation of PC Lamellar Vesicles

PC powder (30 mg) was dispersed into distilled water (1 mL) and sonicated at room temperature until floating substances changed to gel-like precipitates. The gel-like precipitates recovered by centrifugation were suspended in distilled water (200 µL) containing Coomassie brilliant blue (CBB: 20 µg) and incubated for three days at 4 °C to prepare the CBB-containing PC lamellar vesicles. The CBB-containing PC lamellar vesicles were then washed with distilled water via centrifugation until the supernatant changed to a clear fluid. Finally, optical densities of the CBB-containing PC lamellar vesicle suspension were adjusted using distilled water to 2.0 at a wavelength of 660 nm.

2.11 Assay of Structure Collapse-Induction Activity of VDP1, VD2-1 and VD3-7 to PC Lamellar Vesicles

CBB-containing PC lamellar vesicle suspension (200 µL) was incubated for 5 min at room temperature without shaking in the presence or absence of each ethanol (10 µL)-solubilized vitamin D decomposition product (100 µg) and a VDP1 derivative (100 µg). After PC lamellar vesicles were removed by centrifugation, the absorbance ($A_{590\ nm}$) of the supernatant (150 µL) was measured at a wavelength of 590 nm. Collapse indexes of PC lamellar vesicles in the presence of each vitamin D decomposition product and a VDP1 derivative were calculated by relative $A_{590\ nm}$ against the $A_{590\ nm}$ in the absence of those products. Incidentally, we used a 21% hydrochloric acid as the positive control and confirmed that the 21% hydrochloric acid completely causes the collapse of all lamellar vesicles prepared with PC molecular species examined.

2.12 Statistical Significance Analysis

Statistical significance was evaluated by a Student's *t*-test. Difference ($p < 0.01$ and $p < 0.05$) of statistical significance was calculated by the data obtained from independent experiments that were repeated three times.

3. Results

3.1 Cell Injury Activity of VDP1 and VD2-1 to MKN45 Cells and Vero Cells

We first examined the cell injury activity of VDP1 and VD2-1 in MKN45 cells and Vero cells. After MKN45 cells and Vero cells were incubated for 24 h in the presence of either VDP1 or VD2-1 at various concentrations, the viabil-

ity of the cells was measured by an MTT assay. In MKN45 cells, VDP1 and VD2-1 rapidly caused a decline in cell viability at the 40 µg/mL and 30 µg/mL concentrations, respectively, and almost completely abolished the cell viability at the 70 µg/mL concentration (Fig. 2A). Meanwhile, in Vero cells, VDP1 and VD2-1 rapidly decreased cell viability at the 60 µg/mL concentration, and almost completely led to cell death at the 100 µg/mL and 80 µg/mL concentrations, respectively. IC_{50} of VDP1 and VD2-1 were 39.1 $\pm$ 1.6 µg/mL and 29.3 $\pm$ 3.4 µg/mL, respectively, for the viability of MKN45 cells. Meanwhile, IC_{50} of VDP1 and VD2-1 were 62.9 $\pm$ 1.3 µg/mL and 55.9 $\pm$ 0.7 µg/mL, respectively, for the viability of Vero cells. Intriguingly, IC_{50} of VDP1 and VD2-1 for MKN45 cells were statistically lower than those of VDP1 and VD2-1 for Vero cells (Fig. 2B). Hence, MKN45 cells were more sensitive to the cell injury activity of VDP1 and VD2-1 than Vero cells. These results suggest the possibility that the difference in sensitivity to the cell injury activity of VDP1 and VD2-1 between MKN45 cells and Vero cells is due to differences in glycerophospholipid compositions in the biomembranes of these cells.

3.2 Analysis of Lipids of MKN45 Cells and Vero Cells

We next extracted whole lipids from MKN45 cells and Vero cells by an organic solvent distribution method and analyzed lipids by TLC with chloroform–methanol–acetone–water (10:10:1:1) solvents. As a consequence, differences in the detection levels were obviously observed in lipids with high polarity. In the TLC analysis using a Dittmer's reagent, lipids with high polarity turned out to be phospholipids (PL1 and PL2). PL1 was detected with denser staining in MKN45 cells than in Vero cells, while PL2 was detected with denser staining in Vero cells than in MKN45 cells (Fig. 3A). Meanwhile, PL3, PL4 and PL5 were not observed with a conspicuous difference in the qualitative detection between MKN45 cells and Vero cells. After PL1 and PL2 were purified from whole lipids extracted from either MKN45 cells or Vero cells by silica gel-column chromatography with an acetone–methanol solvent system, purified PL1 and PL2 were subjected to a proton nuclear magnetic resonance (^{1}H-NMR) in order to identify those phospholipids (Fig. 3B,C). As a consequence, signals of chemical shifts detected in PL1 and PL2 almost corresponded with the signals of chemical shifts detected in DMPC used as a comparative control phospholipid in ^{1}H-NMR analysis. In sum, PL1 and PL2 turned out to be clusters of PC molecules that differ in polarity. PC is the most prevalent glycerophospholipid composing biomembranes of eukaryotic cells, but individual PC molecules possess fatty acid sidechains with different carbon chain lengths. These results suggest the possibility that the difference in polarities in PC molecules is due to the difference in carbon chain lengths of fatty acid sidechains in PC molecules.

3.3 Fatty Acid Composition of PC of MKN45 Cells and Vero Cells

Next, we analyzed fatty acid composition of PC (PL1 and PL2) purified from either MKN45 cells or Vero cells. After fatty acid methyl esters obtained by methanolysis of PC were separated via a cyanopropyl-silphenylene siloxane column using a palmitic acid-d_{31} methyl ester as the internal standard, the individual fatty acid methyl esters were detected as spectra by an electron ionization mass spectrometry. Each spectrum of fatty acid methyl ester was verified against the spectra of fatty acid methyl esters registered in the computer database library, and fatty acids were identified. The percentage of each fatty acid was calculated by the magnitude of the peak area of the spectrum detected by the gas chromatography/mass spectrometry (GC/MS). As a consequence, PC of MKN45 cells possessed saturated fatty acid (14:0, 16:0, and 18:0) with a higher percentage than PC of Vero cells (**Supplementary Table 1**). Especially, the percentage of myristic acid (14:0) in MKN45 cells' PC was approximately 2.7-fold higher than that of myristic acid in Vero cells' PC. Apart from this, the percentage of palmitoleic acid (16:1) in MKN45 cells' PC was approximately 2-fold higher than that of palmitoleic acid in Vero cells' PC. Conversely, PC of Vero cells possessed unsaturated fatty acid (18:1, 18:2, and 20:1) with a higher percentage than PC of MKN45 cells. Percentages of linoleic acid (18:2) and eicosenoic acid (20:1) of Vero cells' PC were approximately 2-fold and 3.5-fold higher, respectively, than those of linoleic acid and eicosenoic acid of MKN45 cells' PC.

3.4 Analysis of PC Molecular Species of MKN45 Cells and Vero Cells

We next examined PC molecular species of MKN45 cells and Vero cells. After purified PC was separated into individual PC molecules via a C8 column using DMPC-d_{54} as the internal standard, each PC molecule was detected as a spectrum by an electrospray ionization mass spectrometry in negative mode. PC molecular species were determined based on mass spectra of PC molecules, and the data of fatty acid composition were shown in **Supplementary Table 1**. The percentage of each PC molecular species was determined by the magnitude of the peak area of the spectrum detected by the liquid chromatography/mass spectrometry (LC/MS). As a consequence, MKN45 cells contained greater amounts of myristoyl-PC (14:0) molecular species than Vero cells (**Supplementary Table 2**). Palmitoyl-PC (16:0) molecular species had almost equal contents between MKN45 cells and Vero cells. The percentage of palmitoleoyl-PC (16:1) molecular species in total PC was somewhat higher in MKN45 cells than in Vero cells. Meanwhile, Vero cells contained greater amounts of oleoyl-PC (18:1) molecular species than MKN45 cells. For instance, the contents of DMPC were approximately 3.5-fold higher in MKN45 cells than in Vero cells. The total contents of dipalmitoyl-PC (DPPC) and dipalmitoleoyl-PC

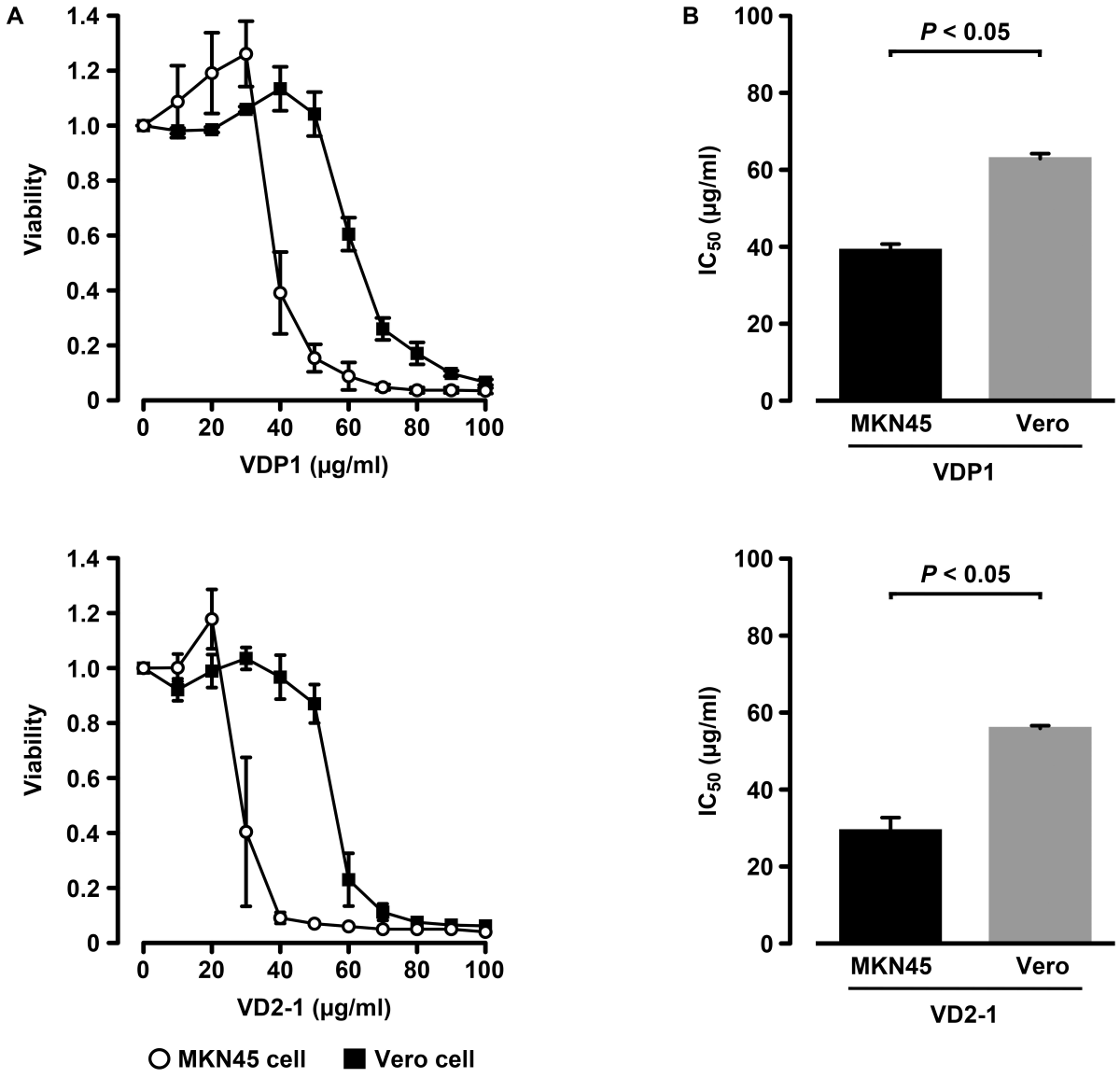

Fig. 2. Cell injury activity of VDP1 and VD2-1 to MKN45 cells and Vero cells. (A) Cell suspension was incubated for 24 h in the presence of various concentrations of either VDP1 (upper panel) or VD2-1 (lower panel). After the incubation, an MTT reagent was added to the cell culture, and incubated for 2 h under the same conditions. After the cell supernatant was removed, MTT metabolites, formazan blue crystallizing only in viable cells, were solubilized in an isopropanol solution containing 5% formic acid, and the absorbance ($A_{540\ nm}$) of the formazan blue solution was measured at a wavelength of 540 nm. Viability of the cells in the presence of each vitamin D decomposition product was calculated by relative $A_{540\ nm}$ against the $A_{540\ nm}$ in the cells in the absence of those products. Data were denoted with the mean value $\pm$ standard deviation obtained from three independent experiments. (B) Based on the results in panel A, IC_{50} was calculated, and a statistically significant difference ($p < 0.05$) was evaluated by a Student's *t*-test. MTT, 3-(4,5-di-methylthiazol-2-yl)-2,5-diphenyltetrazolium bromide; IC_{50}, half maximum inhibitory concentrations.

were almost equal between MKN45 cells and Vero cells. Conversely, the contents of dioleoyl-PC (DOPC) were approximately 1.6-fold higher in Vero cells than in MKN45 cells. In sum, taken together with **Supplementary Tables 1,2**, MKN45 cells turned out to abundantly possess PC molecular species with shorter fatty acid sidechains than Vero cells, and conversely, Vero cells turned out to abundantly possess PC molecular species with longer fatty acid sidechains than MKN45 cells (Fig. 4A).

3.5 Structure Collapse-Induction Activity of VDP1 and VD2-1 to PC Lamellar Vesicles

Next, the structure collapse-induction activity of VDP1 and VD2-1 to PC lamellar vesicles was examined. PC lamellar vesicles containing CBB were prepared with either DMPC, DPPC or DOPC (Fig. 4B), and CBB-containing PC lamellar vesicles were incubated for 5 min in the presence or absence of either VDP1 or VD2-1. Af-

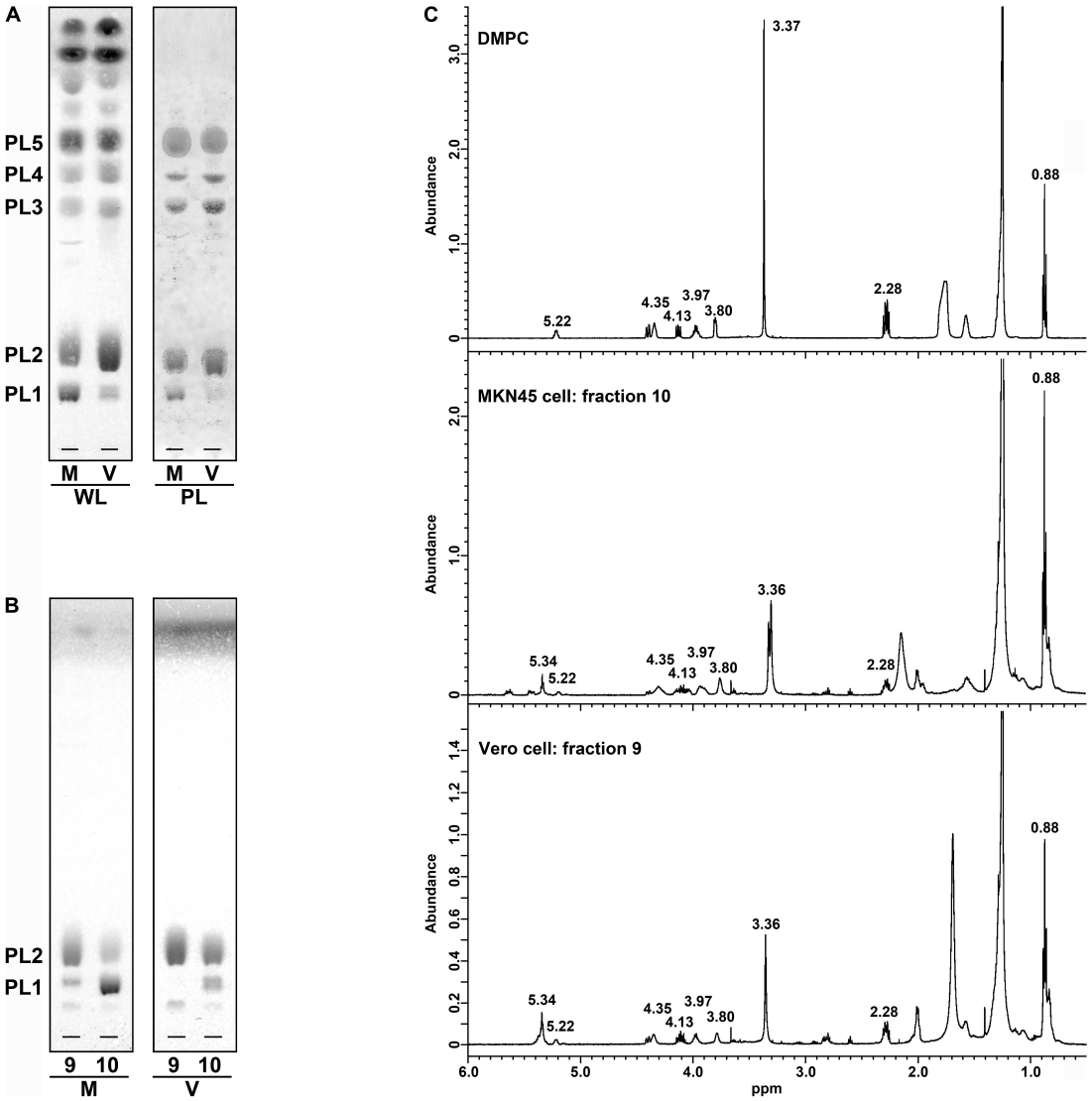

Fig. 3. Analysis of lipids extracted from MKN45 cells and Vero cells. (A) Lipids dotted onto a silica gel plate for TLC were developed on the plate surface together with chloroform–methanol–acetone–water (10:10:1:1) mixture solvents and dried. After a 60% sulfuric acid solution was sprayed on the TLC plate surface, whole lipids were detected by heating the TLC plate at 180 °C (left panel). Phospholipids were detected by spraying a Dittmer's reagent on the TLC plate surface (right panel). WL, whole lipids; PL, phospholipids; M, MKN45 cells; V, Vero cells. (B) Whole lipids extracted from either MKN45 cells (M) or Vero cells (V) were fractionated by silica gel column chromatography with an acetone–methanol solvent system, and phospholipids (PL1 and PL2) contained in fractions 9 (9) and 10 (10) were detected by TLC analysis using a 60% sulfuric acid solution. (C) Chemical shift-signals of DMPC, PL1 (fraction 10) purified from MKN45 cells' lipids and PL2 (fraction 9) purified from Vero cells' lipids were detected by ^{1}H-NMR. TLC, thin layer chromatography; DMPC, 1,2-dimyristoyl-*sn*-glycero-3-phosphocholine.

ter the incubation, the strengthen of the structure collapse-induction activity of VDP1 and VD2-1 to each PC lamellar vesicle was calculated as a collapse index by measurement of CBB levels eluted from PC lamellar vesicles. As a consequence, VDP1 and VD2-1 induced structural collapse to the lamellar vesicles composed of either DMPC or DPPC, while these vitamin D decomposition products induced almost no structural collapse to the lamellar vesicles composed of DOPC (Fig. 4C).

3.6 Cell Injury Activity of VD3-7 to MKN45 Cells and Vero Cells

We next examined the cell injury activity of a VDP1 derivative VD3-7 to MKN45 cells and Vero cells (Fig. 5A). Intriguingly, VD3-7 had no influence on the viability of Vero cells but exhibited the significant cell injury activity to MKN45 cells (Fig. 5B). IC_{50} was a 45.2 $\pm$ 1.9 µg/mL in MKN45 cells and was much higher than 100 µg/mL in Vero cells. Next, we examined the structure collapse-induction activity of VD3-7 to the lamellar vesicles prepared with ei-

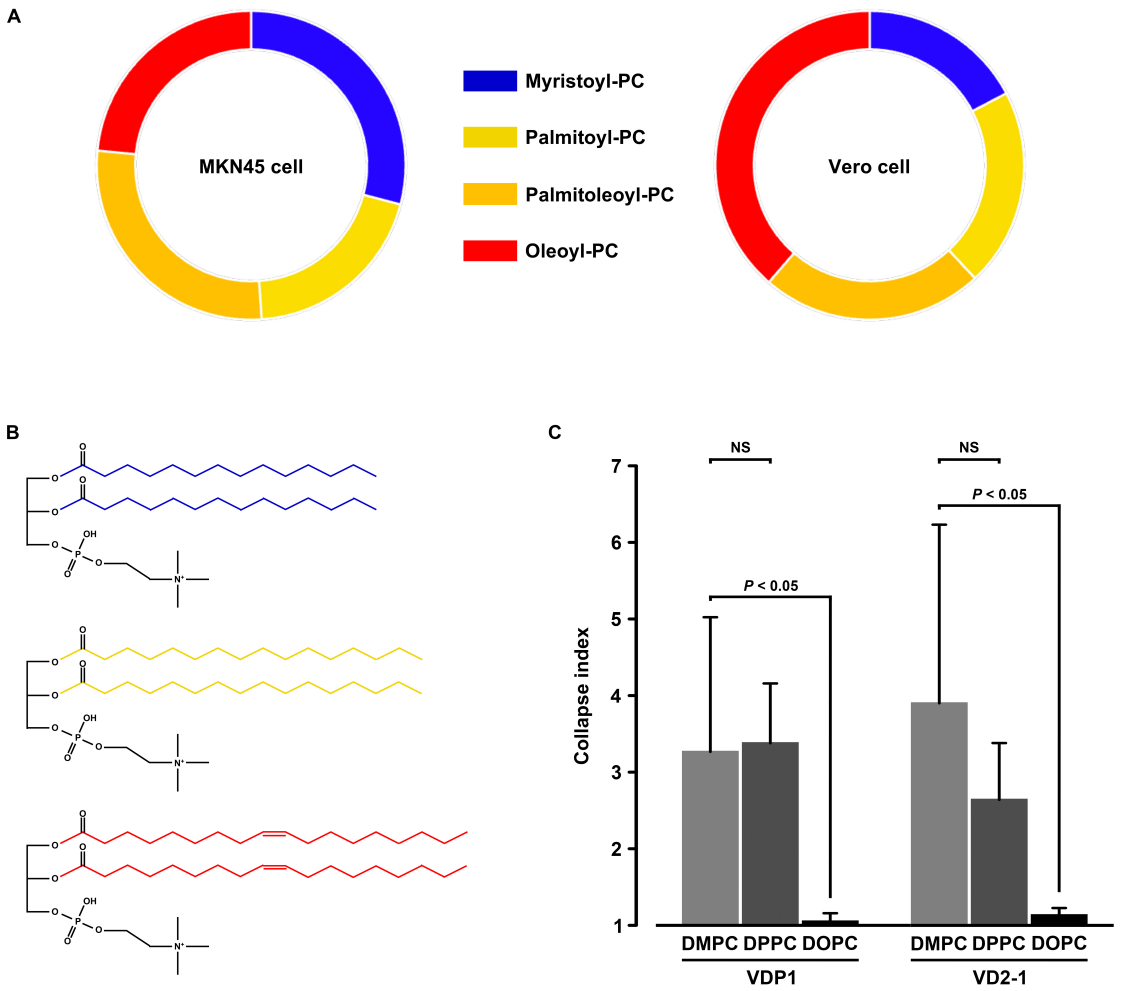

Fig. 4. PC molecular species composition of MKN45 cells and Vero cells, and Structure collapse-induction activity of VDP1 and VD2-1 to PC lamellar vesicles. (A) PC molecular species composition of MKN45 cells and Vero cells. (B) Chemical structures of DMPC (upper), DPPC (middle) and DOPC (lower). (C) After CBB-containing lamellar vesicles prepared with either DMPC, DPPC or DOPC were incubated for 5 min in the solution (200 µL) containing either VDP1 (100 µg) or VD2-1 (100 µg), the absorbance ($A_{590\ nm}$) of the supernatant was measured at a wavelength of 590 nm. The collapse index was calculated by the relative $A_{590\ nm}$ of supernatant in CBB-containing PC lamellar vesicles incubated in the presence of either VDP1 or VD2-1 against the $A_{590\ nm}$ of supernatant in CBB-containing PC lamellar vesicles incubated without VDP1 and VD2-1. Data were denoted with the mean value ± standard deviation obtained from three independent experiments, and statistical significance difference ($p < 0.05$) was evaluated by a Student's *t*-test. NS, no statistical significance. DPPC, dipalmitoyl-phosphatidylcholine; DOPC, dioleoyl-phosphatidylcholine; CBB, Coomassie brilliant blue; PC, phosphatidylcholine.

ther DMPC, DPPC or DOPC. As with the case of VDP1 and VD2-1, VD3-7 also induced the structure collapse to the DMPC and DPPC lamellar vesicles but almost no structure collapse to the DOPC lamellar vesicles (Fig. 5C). These results imply the development of a novel antitumor medicine using a vitamin D decomposition product as the fundamental structure.

4. Discussion

In the case of dimyristoyl-phosphatidylethanolamine (DMPE) and dipalmitoyl-PE (DPPE), VDP1 and VD2-1 exhibit selective structure collapse-induction activity not to the DPPE lamellar vesicles but to the DMPE lamellar vesicles [6,7,9]. In addition to the hydrophobic interaction between an alkyl of vitamin D decomposition products and fatty acid sidechains of PE, electrostatic attraction between a carbonyl of vitamin D decomposition products and a phosphate head moiety of PE plays an important role in the intermolecular interaction between those compounds. On this basis, the lack of selectivity in the structure collapse-induction activity of VDP1 and VD2-1 to the DMPC lamellar vesicles may be due to the phosphorylcholine conformation in a PC molecule. Meanwhile, a previous study by our group elucidated that VD3-7 weakened both the antibacterial activity against *H. pylori* and the

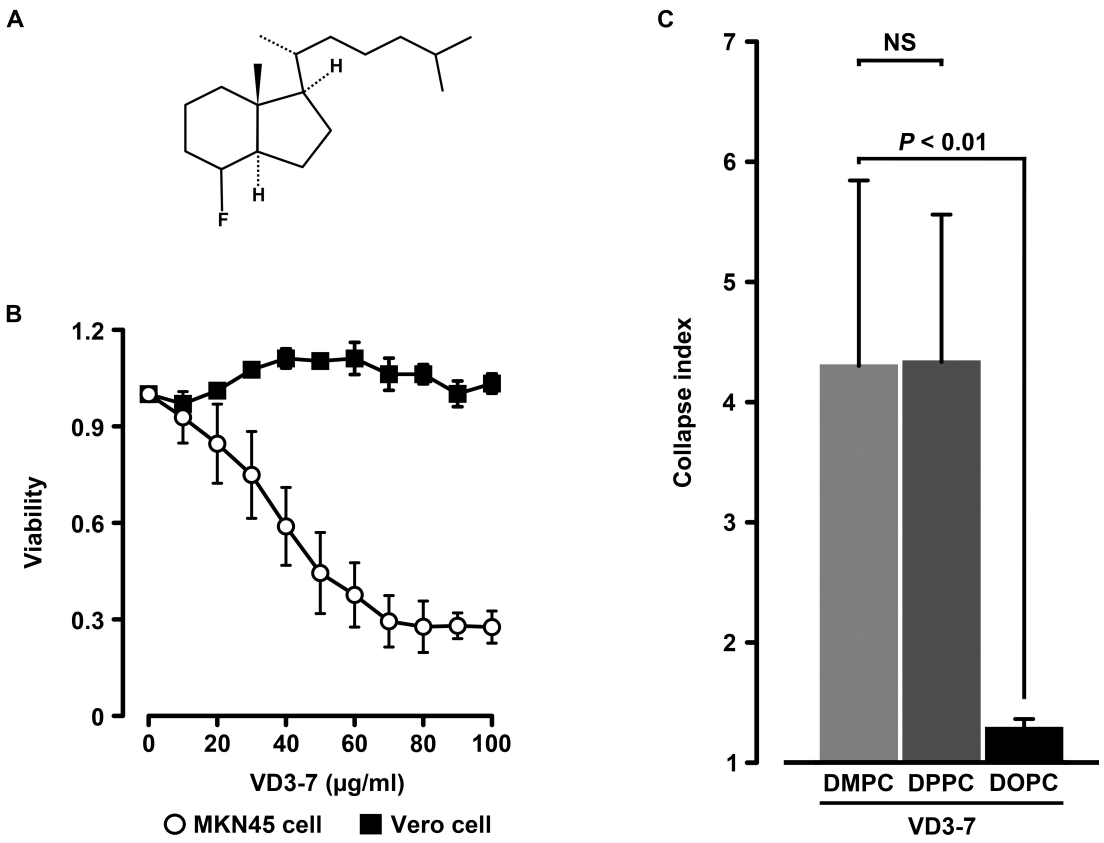

Fig. 5. Cell injury activity of VD3-7 to MKN45 cells and Vero cells. (A) Chemical structure of VD3-7, (1R,7aR)-4-fluoro-7a-methyl-1-((R)-6-methylheptan-2-yl)octahydro-1H-inden. (B) MTT assay was carried out using a VD3-7 by the same method described in Fig. 2A. (C) The structure collapse-induction activity of VD3-7 was evaluated by the same method described in Fig. 4C. Data were denoted with the mean value ± standard deviation obtained from three independent experiments, and statistical significance difference ($p < 0.01$) was evaluated by a Student's *t*-test. NS, no statistical significance.

structure collapse-induction activity against DMPE lamellar vesicles [7]. However, in this study, VD3-7 exhibited the selective cell injury activity to MKN45 cells and exerted the structure collapse-induction activity to DMPC lamellar vesicles. These results mean the possibility that a fluorine in the VD3-7 molecule is the functional group selectively interacting with a phosphorylcholine moiety of PC. In the future, we will need to develop more accurate assay methods for evaluating the structure collapse-induction activity of vitamin D decomposition products and their derivatives on the PC lamellar vesicles and to determine the optimal functional group to selectively act on the phosphorylcholine moiety of PC. Meanwhile, as with the dioleoyl-PE (DOPE) lamellar vesicles, VDP1, VD2-1 and VD3-7 induced almost no structural collapse of DOPC lamellar vesicles. It is not well understood as to why VDP1, VD2-1 and VD3-7 exhibit no structure collapse-induction activity to the DOPE and DOPC lamellar vesicles, but these vitamin D decomposition products and a VDP1 derivative are predicted to be incapable of causing the structural change in the long fatty acid sidechains regardless of the structures of the phosphate head moiety of glycerophospholipids.

Previous studies by our group demonstrated that VDP1 and VD2-1 confer a specific bacteriolytic action to the bacteria that retain myristoyl-PE as the most predominant biomembranal lipid components, while these vitamin D decomposition products confer no bacteriolytic action to the bacteria that retain palmitoyl-PE as the most predominant biomembranal lipid components. On this basis, VDP1 and VD2-1 are considered to target the myristic acid sidechain in a PE molecule, to induce the structural change to its fatty acid sidechain, to thereby destabilize the membrane construction and to ultimately lyse the bacterial cells [1,8]. As shown in Fig. 4A, MKN45 cells contained myristoyl-PC (14:0) in more abundance than Vero cells, whereas Vero cells contained oleoyl-PC (18:1) in more abundance than MKN45 cells. Based on IC_{50}, the susceptibilities of MKN45 cells to the cell injury activity of VDP1 and VD2-1 were approximately 1.6-fold and 1.9-fold higher, respectively, than those of Vero cells to the cell injury activity of the same vitamin D decomposition products. Meanwhile, the percentage of myristoyl-PC in total PC contents in MKN45 cells was approximately 1.7-fold higher than that of myristoyl-PC in total PC contents in Vero cells.

On this basis, the susceptibility of eukaryotic cells to the cell injury activity of VDP1 and VD2-1 seems to be associated with the contents of myristoyl-PC in the biomembranes. In addition, the percentage of oleoyl-PC in total PC contents in Vero cells was approximately 1.6-fold higher than that of oleoyl-PC in total PC contents in MKN45 cells. This means the possibility that oleoyl-PC decreases the susceptibility to the cell injury activity of VDP1 and VD2-1 in Vero cells by preventing of interaction between those vitamin D decomposition products and biomembrane myristoyl-PC. In the future, we will need to clarify the intermolecular interaction between VDP1, VD2-1 and PC molecular species and to elucidate the mechanism for the eukaryotic cell disorder activity of vitamin D decomposition products. In addition, we will also need to analyze whether other phospholipids (PL3 to PL5) are biomembrane lipid components involved in the cell injury activity of VDP1 and VD2-1 to MKN45 cells and Vero cells.

5. Conclusions

Previous studies by our group revealed a unique antibacterial activity of VDP1 and VD2-1 to *H. pylori*, a gastrointestinal pathogen for humans. These vitamin D decomposition products specifically disordered the lipid bilayers of *H. pylori*, followed by bacteriolysis. Direct target of VDP1 and VD2-1 is considered to be a myristic acid sidechain of myristoyl-PE (especially DMPE) contained in the lipid bilayers. In this study, we examined the cell injury activity of VDP1 and VD2-1 in a gastric cancer cell line and a non-cancer cell line. As a consequence, VDP1 and VD2-1 were considered to interact at least with myristoyl-PC in the lipid bilayer of these cell lines and to confer the cell injury action to those cells. In eukaryotic cells, the contents of myristoyl-PC in the biomembranes appeared to be associated with the susceptibility to the cell injury activity of VDP1 and VD2-1. Actually, a VDP1 derivative, VD3-7, significantly exhibited the cell injury activity not to non-cancer cells but to gastric cancer cells with contained high levels of myristoyl-PC. This implies the possibility that VD3-7 reacts more sensitively to the difference in myristoyl-PC contents in the biomembranes. A previous study by another group elucidated that breast cancer cells possess glycerophospholipids with a shorter fatty acid sidechain, such as myristic acid, in more abundance than non-cancer cells [10]. These results mean the possibility that not only gastric cancer cells but also breast cancer cells exhibit high susceptibility to the cell injury activity of VDP1 and VD2-1. In the future, the development of novel medicines using vitamin D decomposition products will be expected in both fields of R&D of antibacterial agents and antitumor agents, targeting a characteristic glycerophospholipid in the biomembranes of pathogenic bacteria and cancer cells.

Abbreviations

VDP1, (1R,3aR,7aR)-1-[(1R)-1,5-dimethylhexyl]octahydro-7a-methyl-4*H*-inden-4-one; VD2-1, (1*R*,3a*R*,7a*R*)-1-((2*R*,*E*)-5,6-dimethylhept-3-en-2-yl)-7a-methyloctahydro-4*H*-inden-4-one; VD3-7, (1R,7aR)-4-fluoro-7a-methyl-1-((R)-6-methylheptan-2-yl)octahydro-1H-inden.

Availability of Data and Materials

The datasets used and analyzed during the current study are available from the corresponding author on reasonable request.

Author Contributions

Conceptualization, HS, MS, and SH; Methodology, HS and KW; Validation, HS and KW; Formal analysis, HS, KW, KH and AA; Investigation, HS, KW, KH and AA; Resources, MS and SH; Writing—original draft preparation, HS; Writing—review and editing, KW, MS and SH; Funding acquisition, HS, KW, KH and MS. All authors contributed to editorial changes in the manuscript. All authors read and approved the final manuscript. All authors have participated sufficiently in the work and agreed to be accountable for all aspects of the work.

Ethics Approval and Consent to Participate

Not applicable.

Acknowledgment

We deeply appreciate Yuichi Ishida of Vaxxinova K. K., who kindly provided us with Vero cells.

Funding

This work was supported by a Grant-in-Aid from Adaptable and Seamless Technology Transfer Program through Target-driven R&D (A-STEP), JSPS KAKENHI, Grant Number 23K04952.

Conflict of Interest

All authors declare no conflicts of interest. One of the authors belongs to Terumo Co., Tokyo, Japan, but the judgments in data interpretation and writing were not influenced by this relationship. In addition, all authors received no sponsorship from this company.

Supplementary Material

Supplementary material associated with this article can be found, in the online version, at https://doi.org/10.31083/FBL45142.

References

[1] Shimomura H, Wanibuchi K, Hosoda K, Amgalanbaatar A, Shoji M, Hayashi S. A short review: the biological activity of vitamin D and its decomposition products. Molecu-

lar Biology Reports. 2025; 52: 214. https://doi.org/10.1007/s11033-025-10322-8.

[2] Warren JR, Marshall B. Unidentified curved bacilli on gastric epithelium in active chronic gastritis. Lancet (London, England). 1983; 1: 1273–1275.

[3] Fukase K, Kato M, Kikuchi S, Inoue K, Uemura N, Okamoto S, *et al*. Effect of eradication of Helicobacter pylori on incidence of metachronous gastric carcinoma after endoscopic resection of early gastric cancer: an open-label, randomised controlled trial. Lancet (London, England). 2008; 372: 392–397. https://doi.org/10.1016/S0140-6736(08)61159-9.

[4] Stolte M, Bayerdörffer E, Morgner A, Alpen B, Wündisch T, Thiede C, *et al*. Helicobacter and gastric MALT lymphoma. Gut. 2002; 50: III19–III24. https://doi.org/10.1136/gut.50.suppl_3.iii19.

[5] Hosoda K, Shimomura H, Wanibuchi K, Masui H, Amgalanbaatar A, Hayashi S, *et al*. Identification and characterization of a vitamin D_3 decomposition product bactericidal against Helicobacter pylori. Scientific Reports. 2015; 5: 8860. https://doi.org/10.1038/srep08860.

[6] Wanibuchi K, Hosoda K, Ihara M, Tajiri K, Sakai Y, Masui H, *et al*. Indene Compounds Synthetically Derived from Vitamin D Have Selective Antibacterial Action on Helicobacter pylori. Lipids. 2018; 53: 393–401. https://doi.org/10.1002/lipd.12043.

[7] Wanibuchi K, Takezawa M, Hosoda K, Amgalanbaatar A, Tajiri K, Koizumi Y, *et al*. Antibacterial effect of indene on Helicobacter pylori correlates with specific interaction between its compound and dimyristoyl-phosphatidylethanolamine. Chemistry and Physics of Lipids. 2020; 227: 104871. https://doi.org/10.1016/j.chemphyslip.2020.104871.

[8] Shimomura H, Wanibuchi K, Hosoda K, Amgalanbaatar A, Masui H, Takahashi T, *et al*. Unique responses of Helicobacter pylori to exogenous hydrophobic compounds. Chemistry and Physics of Lipids. 2020; 229: 104908. https://doi.org/10.1016/j.chemphyslip.2020.104908.

[9] Wanibuchi K, Hosoda K, Amgalanbaatar A, Ihara M, Takezawa M, Sakai Y, *et al*. Aspects for development of novel antibacterial medicines using a vitamin D_3 decomposition product in Helicobacter pylori infection. The Journal of Antibiotics. 2023; 76: 665–672. https://doi.org/10.1038/s41429-023-00651-w.

[10] He M, Guo S, Li Z. In situ characterizing membrane lipid phenotype of breast cancer cells using mass spectrometry profiling. Scientific Reports. 2015; 5: 11298. https://doi.org/10.1038/srep11298.